International Journal of Electrical, Electronic and Communication Sciences
ISSN: 2517-9438
Vol:1, No:6, 2007

Scanning Device for Sampling the Spatial Distribution of the E-field

Juan Blas, Alfonso Bahillo, Santiago Mazuelas, David Bullido, Patricia Fernández, Rubén M. Lorenzo, and Evaristo J. Abril

***Abstract*—**This paper presents a low cost automatic system for sampling the electric field in a limited area. The scanning area is a flat surface parallel to the ground at a selected height. We discuss in detail the hardware, software and all the arrangements involved in the system operation. In order to show the system performance we include a campaign of narrow band measurements with 6017 sample points in the surroundings of a cellular base station. A commercial isotropic antenna with three orthogonal axes was used as sampling device. The results are analyzed in terms of its space average, standard deviation and statistical distribution.

***Keywords*—**measurement device, propagation, spatial sampling.

I. Introduction

THE spatial distribution of the electric field in urban areas is a key issue in many fields of electrical engineering. Specifically, propagation models are considered for analyzing the wireless communication channel in order to achieve a performance improvement. On the other hand there also exist some concerns about environmental electric and magnetic fields level control and safety guideline compliance. In this sense, measurement campaigns are carried out for guideline compliance assessment purposes.

It is not easy to evaluate the spatial variability of the electric field strength by moving a probe along the measurement plane or volume doing it by hand. For example, wideband measurement systems are especially sensitive to movement. In addition, it is known that there are perturbations of the fields being measured due to the presence of the human body [1]. Given that, if we want to characterize the field in a limited area at some level of detail, we need some automatic system to perform the spatial sampling process by carrying the probe along selected lines that contains the spatial sampling points. At these fixed locations the vehicle that carries the probe stops and performs the measurement process. This scanning device could also choose the next sampling point according to the data recorded in previous steps to decide whether undersample or oversample the next spatial segment.

In this paper we present a low cost spatial scanning device that could be useful for experimental studies. Actually we are employing it to corroborate propagation models, to design positioning algorithms in wireless networks and to assess human exposure to RF sources. Its flexibility and modular design facilitates customization. Its capabilities are shown by means of a narrow band measurement campaign carried out indoors. The measures were taken in the vicinity of a cellular base station, with direct line of sight of the GSM base station antennas.

Juan Blas, Alfonso Bahillo, Santiago Mazuelas and David Bullido are with CEDETEL (Center for the Development of Telecommunications), Parque Tecnológico de Boecillo, Valladolid (SPAIN), email: abahillo@cedetel.es, jblas@cedetel.es, smazuelas@cedetel.es

Patricia Fernandez, Ruben Mateo Lorenzo and Evaristo Jose Abril are with the Department of Signal Theory and Communications and Telematic Engineering, University of Valladolid, Valladolid (SPAIN), email: patfer@tel.uva.es, rublor@tel.uva.es and ejad@tel.uva.es

This research is partially supported by the Regional Ministry of Education from Castilla y Leon (Spain) under grant VA009B06.

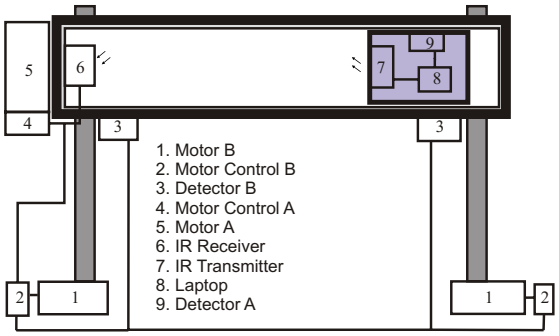

Fig. 1. Block Diagram of the Scanning Device

II. Measurement System

The scanning device is based on a rail-guided vehicle which is moved slowly from the beginning to the end of the rails by using a DC electric motor. This motor is shown on the top left corner in Fig. 1 and is labeled as “5”. It pulls the vehicle in both directions. A pulley is attached to the opposite end of the rails to move the vehicle back to the starting position. The secondary rails are orthogonal to the ones mentioned earlier and much wider. Their aim is to add another dimension to the sampling space: a flat surface parallel to the ground. The motors shown in the bottom of Fig. 1 pull the first rails, which in turn carry the vehicle on them. These two independent motors are shown at the bottom of Fig. 1 and are labeled as “1”.

There are three devices on the vehicle involved in the automatic control of the movement of the vehicle that carries the probe:

- An IR emitter (label “7”) which sends a signal that activates or deactivates the motors (label “5” and labels “1”).
- A positioning system that provides information needed for halting the vehicle when it reaches a sampling point (label “9”).
- A laptop which controls the overall process (label “8”).

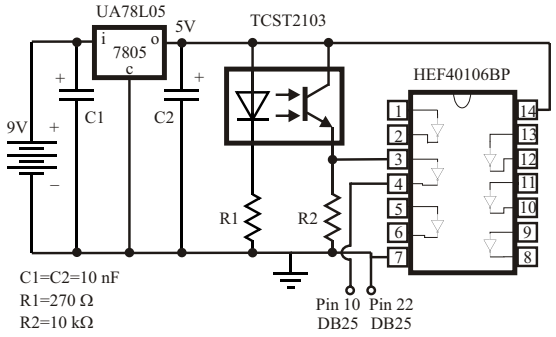

Fig. 2. Vehicle Positioning Subsystem

The laptop is also responsible for commanding the spectrum analyzer and switching among the three orthogonal axes of the isotropic E-field probe in order to perform the measurements once the vehicle has been stopped. All these devices are carried on the vehicle in order to avoid relative movement of the probe to the rest of them.

There are other two detectors fixed to the narrow rails (labels "3") that read the position on the wider rails. They can stop its motor (labels "1") in an autonomous way when a slot in its rail is found.

A. Vehicle positioning

In order to control the movement of the vehicle along its own rails we use a positioning system based on the transmissive optical sensor TCST2103. The sensor is made up of a pair of photoelectric coupled elements that detect narrow slots performed at centimeter intervals in the rail. The led is always switched on but only when it reaches a slot its light is detected by the phototransistor on the other side of the rail. We show the circuit arrangement in Fig. 2. The HEF40106BP inverting Schmitt trigger is needed to avoid spurious oscillations in the output signal that imply a risk of false detections.

At the moment when the positioning subsystem detects one slot, it reports to the laptop that it has to stop the vehicle by changing the logical state of the pin 10 of the parallel port. Then an interrupt request signal is received in the laptop.

B. Primary motor control

The primary motor that pulls the vehicle is controlled by means of the circuit shown in Fig. 3. It has two distinct parts. The first one is a solid state relay that allows the laptop to be used to switch the DC source (model CU10-14) that in turn is going to power the motor. The second part, shown at the bottom of Fig. 3, is based on the L293B driver and is used to reverse the direction of motion of the vehicle. When the vehicle arrives at the end of the rails it pushes a limitswitch. Then the state is stored using an RS bistable (built with HE4001) so the vehicle returns until it finds the other limitswitch. An important tip is that the thread between the motor and the vehicle must not be elastic to avoid that the

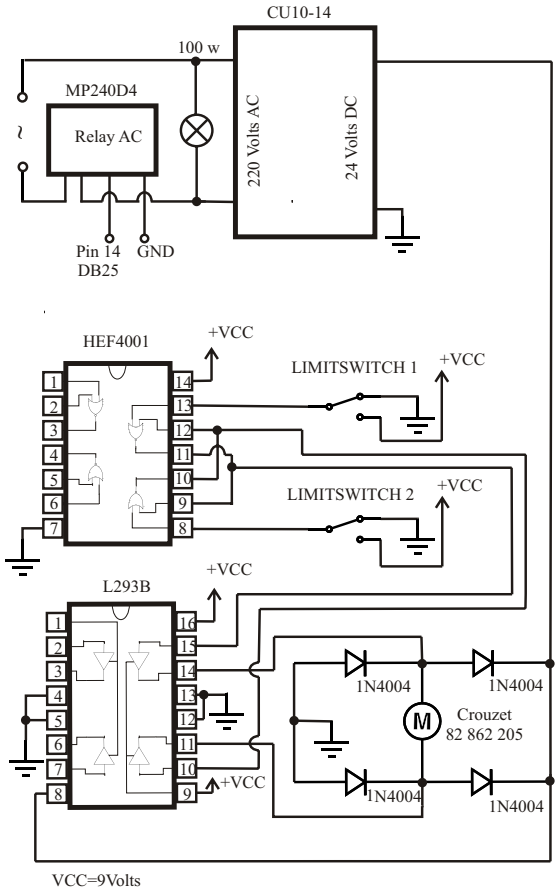

Fig. 3. Primary Motor Control

vehicle keeps moving after halting the motor. For this reason we use a cord of sisal or flax instead of nylon.

C. Positioning system. Secondary motors

The two secondary motors pull the primary rails where the vehicle is standing. Therefore these secondary motors perform the motion in the orthogonal direction to the one obtained with the primary motor. We need a positioning system to stop these motors when the primary rails reach the sampling point. This positioning system is similar to the one attached to the vehicle. However, in this case the circuit itself switches off the motor without any external signal from the laptop, which waits for the vehicle to stop moving by using a time counter.

As it is shown in Fig. 4, we need a RS bistable to store the state. Notice that the motion finishes just when the detector leaves behind the slot (Fig. 5). We use also a L293B driver to control the secondary motors.

D. Infrared link

The laptop must send the ON/OFF signals to the motors. Because of the vehicle motion, a wired solution is not optimal. As a result, we have chosen an infrared link to carry out this connection. In the case of the primary motor we need the

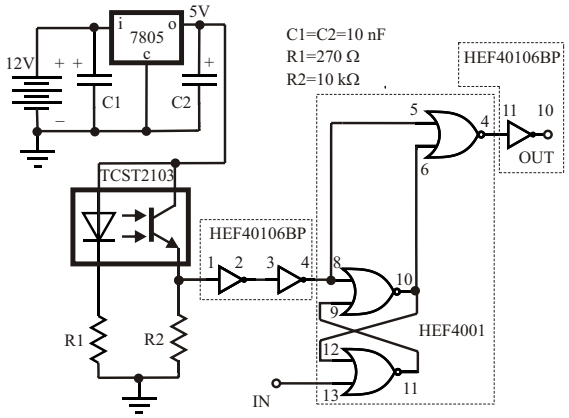

Fig. 4. Secondary Positioning System.

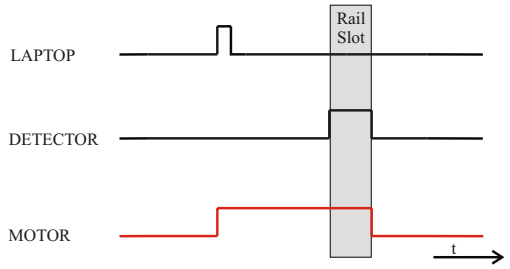

Fig. 5. Output Signal (Motor control)

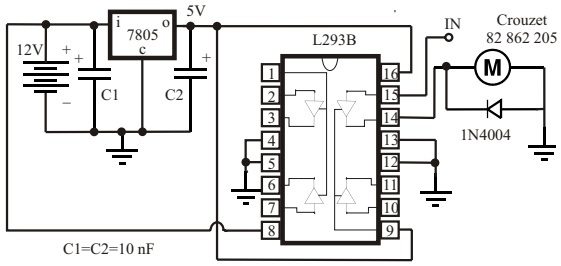

Fig. 6. Secondary Motors Control

signal to stay in the same logic level while the vehicle is moving. On the contrary, the secondary motors just need one short pulse (500 ms) to start the motion and the positioning subsystem itself halts the motor.

The infrared (IR) transmitter and receiver are shown in Fig. 7 and Fig. 8. They are based on HT12E and HT12D, used to modulate and demodulate a 12 bit word (8 bit receiver address plus 4 data bits). In our case, we just needed two bits but we have increased the complexity of the initial design in order to ease future enhancements. The IR emitter is always switched on and the laptop controls the value of the data sent.

E. Triaxial probe control

A triaxial isotropic probe (Insite Free made by Antennessa) is used to measure the E-field strength. Below the probe, on the vehicle, a switch box selects among the three orthogonal axes.

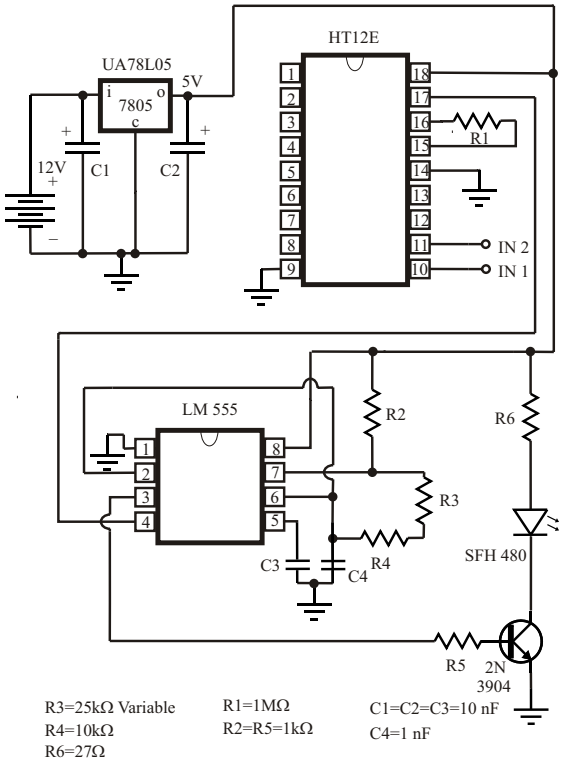

Fig. 7. IR Transmitter

The laptop, also placed on the vehicle, controls the switch box by means of the parallel port: signals from the data register of the parallel port are latched on the switch box, so just short pulses are needed to select the desired polarization axis. The signal is coupled from the triaxial probe to the switch box by means of three coaxial cables. Ferrite beads are mounted on this transmission line to avoid perturbations of the fields by surface currents induced on the cable shield. The switch box is connected by coaxial cable to the spectrum analyzer.

F. Spectrum analyzer control

A spectrum analyzer (R&S FSH3) is placed on the vehicle, adjacent to the switch box. The laptop is communicated with the analyzer through the serial port of the laptop. The analyzer has an optical to serial interface to avoid metallic cables. The control software is written in Microsoft Visual Basic and is based on the VXYPlug&Play driver of the analyzer.

III. Results

Finally we show the measurements carried out in the room shown in Fig. 9. This room was empty, without furniture. It had brick walls, a false ceiling and a tile floor. From its windows it could be seen a typical GSM Base Station (BS) and its panel antennas. The distance from the BS to the windows was approximately 300 m and the direct ray was almost completely horizontal (10 degrees deviation). This obliquely incident ray had an angle of incidence of 60 degrees respect to the window panes.

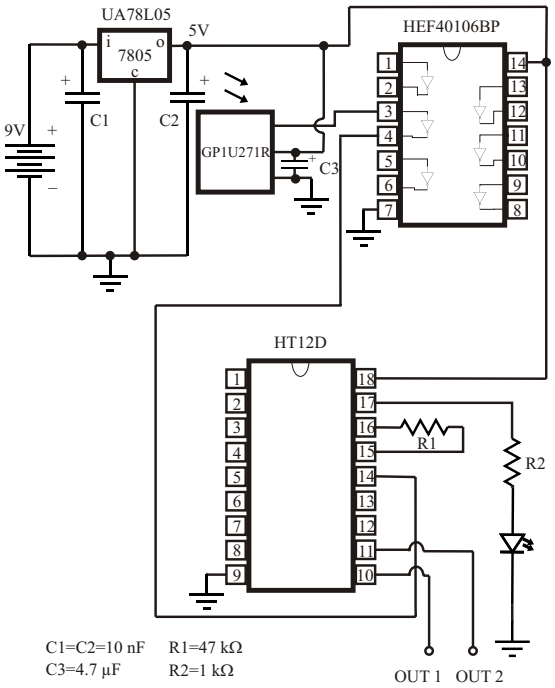

Fig. 8. IR Receiver

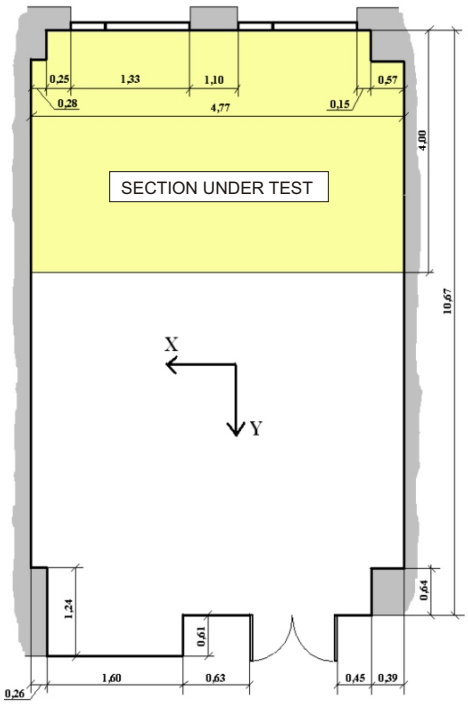

Fig. 9. The Measurement Room

The power of a Broadcast Control Channel (BCCH) was measured because it is transmitted continuously with constant power. As a result, the spatial field patterns are almost stationary waves in our case. It was used Root Mean Square (RMS) detector and 200 kHz resolution bandwidth. Each measure is the arithmetic mean of three consecutive measurements performed in the same point with the same probe.

The measurement points were spaced every 4 cm in the X axis and 7 cm in the Y axis to give a detailed view of the spatial variations of the E-field. The grid was more dense in the X axis because the direct ray was illuminating a lateral wall and it had a dominant role in the stationary pattern of the field distribution.

The E-Field readings are shown in Fig. 10. Each one of the three polarization states is represented in a different data plot. Adjacent to them, in Fig. 11, it can be found a statistical analysis of the data. A log-weibull model is used to fit the data distribution. This model fits better than log-nakagami or log-normal distributions. Similarly in terms of amplitude (a good compilation of models can be found in [2]) a weibull distribution fits better than nakagami or rayleigh distributions.

A physical model for weibull fading can be found in [3], [4]. The importance of 3D polarization concept is explored in [5]. In our case the statistical distribution of two of the polarizations are similar, while the third one is different. It can not be assumed that the attenuation function is independent of the type of polarization. This could be explained by the fact that the angle of incidente of the waves is almost orthogonal to the lateral walls, so there are much more energy reflected on these walls than on the rest.

It is to be noted that at lower spatial sampling rates we could get this kind of information. However, our detailed view of the spatial variations reveals that the local spatial distribution of the E-field has a clear orientation inside the room. The areas with constructive interferences have shapes parallel to the lateral walls. When dealing with mimo channels or studying exposure to radiowaves this spatial patterns should be taken into account to get a more precise understanding of the measurements performed.

IV. Conclusions

A simple 2D automatic scanning system has been developed to characterize the electromagnetic levels in a room situated in the vicinity of a GSM 900 base station and with direct line of sight between the antennas and the room windows.

The stationary pattern due to a BCCH channel has been spatially sampled. The data have been fit using a weibull distribution. We have found that two of the three polarization states had quite similar statistics. Other important point is that the spatial distribution is strongly dependent on wall orientation as can be appreciated in Fig. 10. Finally we have shown that the spatial patterns have shapes related to the wall position.

Even a preliminary study seems to indicate that the three polarization components play an important roll in achieving a proper understanding of the electromagnetic environment. A detailed sampling of the E-Field can reveal stationary patterns that contain a description of the surroundings. All

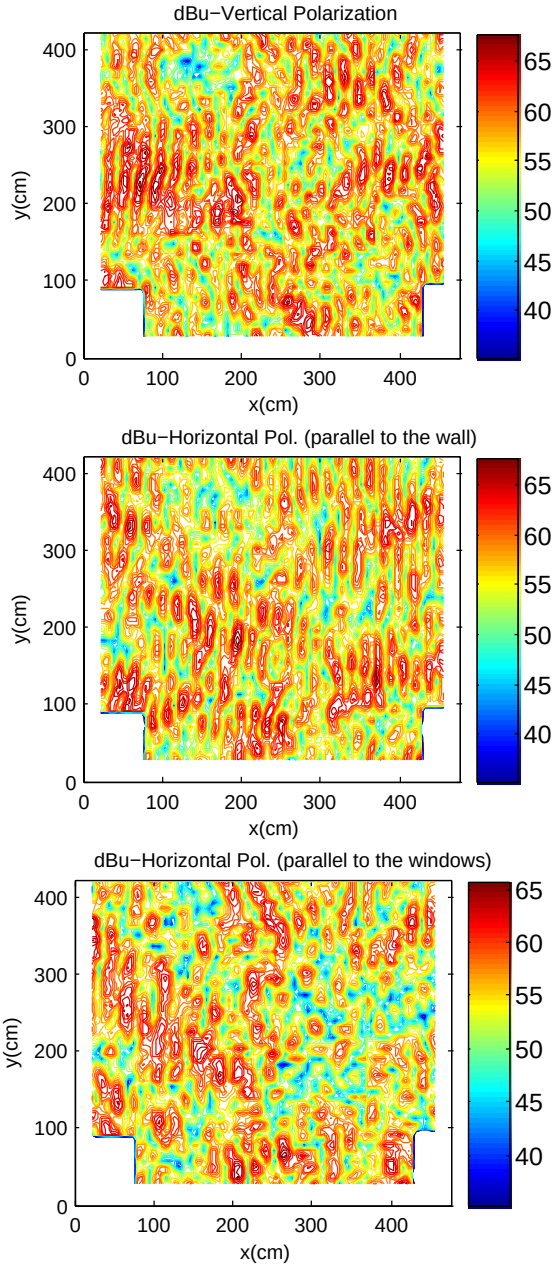

Fig. 10. Spatial Distribution of the E-field

this information is a valuable tool to assess human exposition characteristics and also to improve the performance of new radio communication systems.

REFERENCES

[1] J. Blas, F. Lago, P. Fernández, R. Lorenzo, and E. Abril, "Potential exposure assessment errors associated with body-worn rf dosimeters," *Bioelectromagnetics*, accepted for publication.

[2] H. Hashemi, "The indoor radio propagation channel," *Proceedings of the IEEE*, vol. 81, no. 7, pp. 943–968, July 1993.

[3] M. Daoud Yacoub, "The α-μ distribution: a general fading distribution," in *Personal, Indoor and Mobile Radio Communications, 2002. The 13th IEEE International Symposium on*, vol. 2, 15-18 Sept. 2002, pp. 629–633vol.2.

[4] N. Sagias and G. Karagiannidis, "Gaussian class multivariate weibull distributions: theory and applications in fading channels," *Information Theory, IEEE Transactions on*, vol. 51, no. 10, pp. 3608–3619, Oct. 2005.

[5] P. Horváth, G. K. Karagiannidis, P. R. King, S. Stavrou, and I. Frigyes, "Investigations in satellite mimo channel modeling: Accent on polarization," *EURASIP Journal on Wireless Communications and Networking*, vol. 2007, pp. Article ID 98 942, 10 pages, 2007, doi:10.1155/2007/98942.

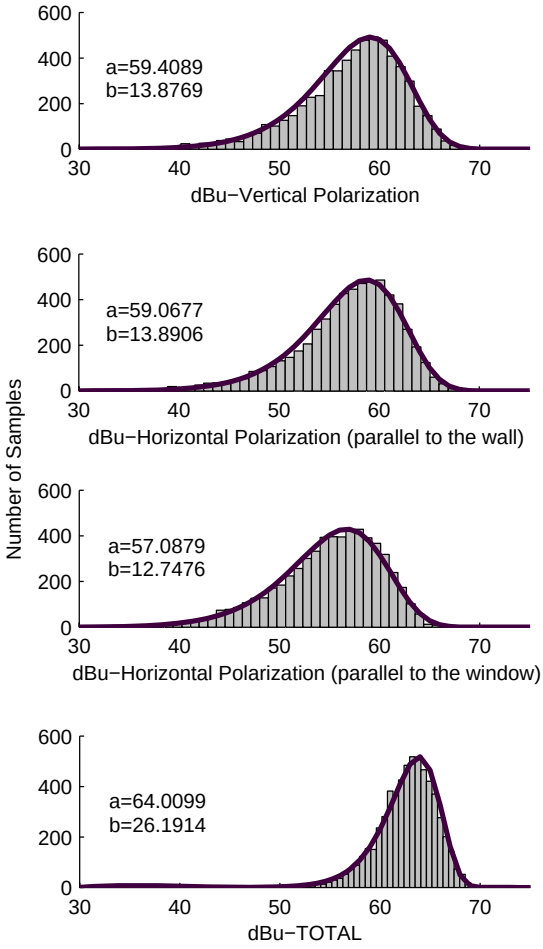

Fig. 11. Histograms